

PASS PREDICTION, MOLECULAR DOCKING AND PHARMACOKINETIC STUDIES OF ACYL-SUBSTITUTED BIOACTIVE GALACTOPYRANOSIDE ESTERS AS ANTIBACTERIAL AGENTS

Sarkar Mohammad Abe Kawsar^{1,*}, Mebarka Ouassaf², Samir Chtita³, Aishi Barua Jui¹, Salah Belaidi²

¹ Laboratory of Carbohydrate and Nucleoside Chemistry (LCNC), Department of Chemistry, Faculty of Science, University of Chittagong, Chittagong-4331, Bangladesh

² Group of Computational and Medicinal Chemistry, Laboratory of Molecular Chemistry and Environment Laboratory, University of Biskra, BP 145 Biskra 07000, Algeria

³ Laboratory of Analytical and Molecular Chemistry, Faculty of Sciences Ben M'Sik, Hassan II University of Casablanca, BP7955 Sidi Othmane, Casablanca, Morocco

akawsar@cu.ac.bd

Currently, methyl- β -D-galactopyranoside (MDG) esters have become a focus of attention due to their promising biological and pharmacokinetic properties and could be a good choice in unraveling the global issue of pathogenic multidrug resistance. Structural modification of MDG can improve its mode of biological activity. In line with these efforts, a series of previously synthesized MDG esters were designed and evaluated by Prediction of Activity Spectra for Substances (PASS), molecular docking simulation, and pharmacokinetic depiction. Encouraging PASS activity was observed for several aliphatic and aromatic MDG esters, and antibacterial efficacy was more promising than other features. In support, molecular docking studies were performed against the macrolide phosphotransferase enzyme MPH to identify a potential allosteric binding site for these esters. Molecular docking indicated that the shape of the MDG esters and their ability to form multiple electrostatic and hydrogen bonds with the active site corresponds to the binding modes of other minor-groove binders. Pharmacokinetic predictions were also performed to evaluate the absorption, metabolism, and toxic properties of MDG esters. These findings demonstrate that MDG esters are promising for use as biocompatible antibacterial agents in the future.

Keywords: methyl- β -D-galactopyranoside; MDG; molecular docking; antibacterial agent; pharmacokinetics; PASS

ПРЕДВИДУВАЊА СО PASS, МОЛЕКУЛСКО ПРИПОЈУВАЊЕ И ФАРМАКОКИНЕТИЧКИ ИСПИТУВАЊА НА БИОАКТИВНИ ГАЛАКТОПИРАНОЗИДНИ ЕСТЕРИ СУПСТИТУИРАНИ СО АЦИЛ КАКО АНТИБАКТЕРИСКИ СРЕДСТВА

Во последно време естерите на метил- β -D-галактопиранозид (MDG) се во фокусот на внимание поради нивните потенцијални биолошки и фармакокинетички својства и можно е да се на добар пат да го решат глобалниот проблем на отпорноста на патогени микроорганизми спрема повеќе лекови. Структурни промени на MDG можат да ја подобри неговата биолошка активност. Во согласност со овие напори беа дизајнирани и евалуирани серија претходно синтетизирани естери на MDG со предвидување на спектри на активност на супстанции (PASS), со симулација на молекулско припојување, како и со фармакокинетички испитувања. Беше добиена надежна активност на PASS за неколку алифатични и ароматични естери на MDG при што најистакната беше антибактериската ефикасност. За поддршка беа изведени и студии на молекулско припојување со микролиден фосфоропреносен (MPH) ензим за да се идентификува потенцијална алостерна положба за спојување на овие естери. Молекулското припојување укажува дека обликот на естерите на MDG и нивната способност да образуваат повеќе електростатични и водородни врски

со активен центар соодветствува на начините на припојување на други средства за сврзување во помалите жлебови. Беа извршени и фармакокинетички предвидувања за да се одреди апсорпцијата, метаболизмот и токсичноста на овие естери. Овие резултати укажуваат дека естерите на MDG се надежни за употреба како биокомпатиблини антибактериски средства во иднината.

Клучни зборови: метил- β -D-галактопиранозид; MDG; молекуско припојување; антибактериски средства; фармакокинетика; PASS

1. INTRODUCTION

Food contamination caused by microorganism activity has a serious effect on human health, particularly via digestive diseases.^{1,2} With the expansion of the use and abuse of antibiotics, increasing numbers of drug-resistant strains have emerged in the clinic. Common harmful bacteria are *Escherichia coli*, *Staphylococcus aureus*, *Bacillus subtilis*, and *Salmonella typhimurium*, while one example of common harmful fungi is *Aspergillus flavus*.³⁻⁵ To prevent contamination, industries use antimicrobial agents to preserve their products by inhibiting microorganism activity. However, some antimicrobial agents are toxic and are also non-biodegradable, thus raising other problems for human consumption.⁶ The discovery of new drugs is now focused on drug targets such as enzymes or receptors. Macrolide phosphotransferase carrier protein of the *E. coli* species is one of the attractive targets in *E. coli*-associated diseases. Macrolide 2'-phosphotransferase [MPH(2')] was purified 90-fold from an erythromycin-resistant strain of *E. coli*, and its enzymatic properties were investigated and radical changes to the erythromycin scaffold tested.⁷ MPH(2') is an inducible intracellular enzyme that shows high levels of activity with 14-member-ring macrolides and extremely low levels with 16-member-ring macrolides. Again, Gram-negative bacteria comprise the majority of microbes that cause infections and are resistant to pre-existing antibiotics. The complex cell-wall architecture contributes to their ability to form biofilms, which are often implicated in hospital-acquired infections.⁸ Monosaccharide esters have attracted many researchers globally due to their biocompatibility.^{9,10} They are especially developed in the biological and pharmaceutical fields for their antimicrobial, antioxidant, etc. properties.^{11,12} For a long time, carbohydrates have been a very attractive topic for scientists due to their immense importance in biological systems including in viral and bacterial infections, cell growth and proliferation, cell-cell communication as well as immune response.^{13,14} They are the source of metabolic energy supply, but also for the fine-tuning of cell-

cell interactions and other crucial processes. It was found from the literature survey that a large number of biologically active compounds also possess aromatic, heteroaromatic, and acyl substituents.¹⁵⁻¹⁷ The benzene, substituted benzene, and also nitrogen-, sulfur-, and halogen-containing substituents are known to enhance the biological activity of the parent compound.¹⁸⁻²¹ It is also known that if an active nucleus is linked to another active nucleus the resulting molecule may possess greater potential for biological activity.²²⁻²⁶ Moreover, selective acylation of carbohydrates and evaluation of microbial activities reveal that in many cases the combination of two or more heteroaromatic nuclei and acyl groups enhances the biological activity manifold over its parent nucleus. In a recent study, some methyl- β -D-galactopyranoside (MDG) esters are found to be potential inhibitors against cancer cell protein [ADP-ribose] polymerase1.²⁷

Therefore, in the present work, a series of MDG esters were designed to investigate their antimicrobial mode through their biological prediction, molecular docking interaction, and pharmacokinetic and toxicity analysis. Antimicrobial screening was performed for all esters with the prediction of their Prediction of Activity Spectra for Substances (PASS) properties. Further, MDG esters were employed for molecular docking against macrolide phosphotransferase (MPH) enzyme (PDB: 5igi; <http://dx.doi.org/10.1016/j.str.2017.03.007>) to understand their nonbonding interactions, binding mode, and antibacterial efficacy. Finally, pharmacokinetic enumeration was performed to compare their absorption, metabolism, and toxicity. This inherent investigation revealed the potentiality of MDG esters as antibacterial agents that will be of great benefit for future antimicrobial research.

2. EXPERIMENTAL

2.1. PASS prediction

The online web application PASS (<http://www.pharmaexpert.ru/passonline/>) was employed to calculate the antimicrobial activity spectrum of the selected MDG ester.²⁸ Firstly, struc-

tures of the MDG esters were drawn, and then changed into their Simplified Molecular Input Line Entry Specification (SMILES) formats by using SwissADME free online applications (<http://www.swissadme.ch>), which are renowned in determining antimicrobial spectra using the PASS web tool. PASS outcomes are revealed by Pa (probability for active molecule) and Pi (probability for inactive molecule) scores. Having potentialities, the Pa and Pi scores vary in the range 0.00–1.00; usually, $Pa + Pi \neq 1$, as these potentialities are predicted freely.

2.2. Geometry optimization

In computer-based drug design, the calculation of thermal, molecular orbital and molecular electrostatic features are widely performed based on quantum mechanical methods. Geometrical calculations and subsequent alteration of MDG esters were performed employing the Gaussian 09 pro-

gram.²⁹ Optimization of all MDG esters were carried out by employing density functional theory (DFT) force field with Beck's (B) three-feature hybrid model and Lee, Yang and Parr's (LYP) correlation functional, applying the basis set 3–21G.

2.3. Preparation of macromolecule and molecular docking simulation

The antibacterial activity of the synthesized esters was further analyzed by the molecular docking approach. All docking simulations were performed using Molecular Operating Environment software (MOE 10.2004; Chemical Computing Group Inc., Montreal, Quebec, Canada; <http://www.chemcomp.com>). Energy minimizations were carried with an Root-Mean-Square Deviation (RMSD) gradient of $0.05 \text{ kcal mol}^{-1} \text{ \AA}^{-1}$ with an MMFF94X force field, and the partial charges were estimates. Result analysis and visualizations were performed with ligplot+v1.4.5.³⁰

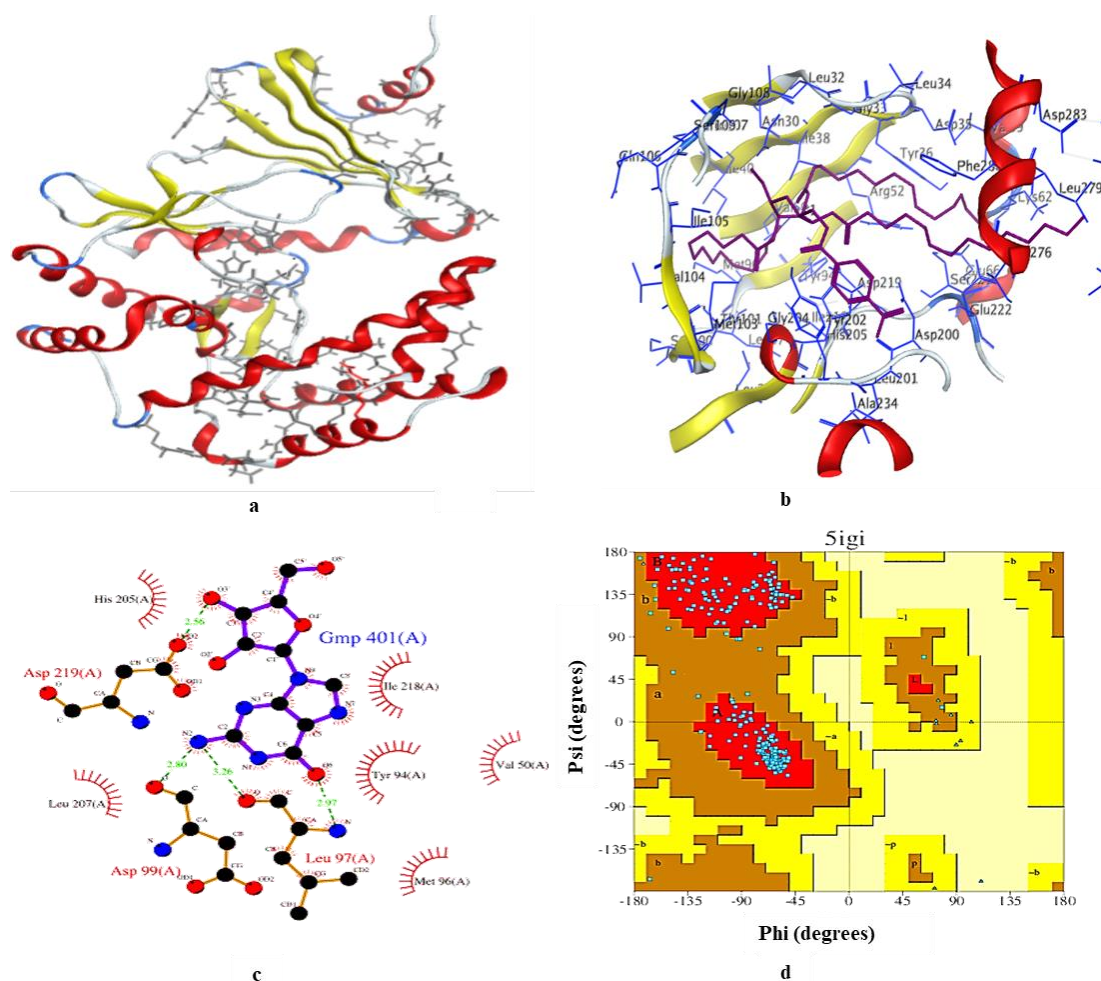


Fig. 1. (a) Three-dimensional structure of the receptor Macrolide 2'-phosphotransferase type I; (b) the MPH macrolide binding site; (c) Ramachandran plot for the macrolide phosphotransferase enzyme (PDB: 5igi); and (d) LigPlot image of the ligand-macrolide phosphotransferase enzyme (PDB: 5igi) complex in 2D view as predicted by PDB sum

The structure of MPH in the docking study was downloaded from Protein Data Bank (PDB: 5igi; Fig. 1a), co-crystallized with azithromycin.³¹ Molecular docking of all esters at the active site of MPH³² was performed to investigate their binding interactions with amino acids (Fig. 1b). The enzyme was prepared for docking studies by removing water molecules and hydrogen atoms that were added to the enzyme. The MOE Site Finder was used to select the active sites in the enzyme along with the elimination of the co-crystallized ligand, and docking was then performed with the designed MDG esters.

For ligand preparation, Marvin Sketch software³³ was used to draw the structure of selected compounds. The structures were converted to 3D and the energy minimized by the MMFF94 function. The triangle matching algorithm was selected from MOE for docking the esters into the active sites of the selected proteins. The PDB sum online server was also used to check the validation of the MPH (PDB: 5igi) with Lig-plot (Fig. 1c) and Ramachandran plot (Fig. 1d), which revealed that 93.70 % residues were in the allowed region and no residues were missed.

2.4. Pharmacokinetic properties and toxicity

The prediction of Absorption, Distribution, Metabolism Excretion and Toxicity (ADMET) properties in drug development is important to prevent drug failure in the clinical stages. For this reason, the best-identified esters were evaluated using pkCSM³⁴ for their *in silico* pharmacokinetic parameters: their absorption in the human intestine, percolation of the blood-brain barrier and the central nervous system, the metabolism, indicating the chemical biotransformation of a drug by the body, their total clearance and the toxicity levels of the molecules. The drug-likeness of a molecule is expressed by Lipinski's rule of five parameters (molecular weight <500 Da, no more than five hydrogen-bond donors, no more than 10 hydrogen-bond acceptors, and logP should not be greater than 5). Lipinski's rule of five properties were ob-

tained from the SwissADME server (www.swissadme.ch/index.php). Prediction of the drug-likeness of the designed MDG esters was also assessed by rule-based filters from Lipinski, Ghose, Veber, and Egan, and the synthetic accessibility difficulty scale was 1–10.

3. RESULTS AND DISCUSSION

In the present study, 11 MDG esters were modified with different aliphatic and aromatic chains (**2–12**; Table 1) and geometrical optimization was attempted to realize their mode of antimicrobial behavior. Initially, biological activities of partially acylated esters were predicted using the PASS web tool. The observed activities were then rationalized by calculating their physicochemical, toxicity, molecular docking properties, in combination with *in silico* pharmacokinetic and drug-likeness properties. Selective alteration of a certain hydroxyl group is important in carbohydrate chemistry because the resulting acylation products might provide useful precursors for the synthesis of novel and bioactive products. Moreover, the designed acyl esters might have great antibacterial effectiveness as versatile intermediates in the synthesis of various other antibacterial drugs of fundamental importance.

3.1. Structural identification of designed MDG esters

Atomic identification and structural variation of substituted MDG esters are displayed in Tables 1 and 2. Different aliphatic (lauroyl and myristoyl) and aromatic (4-bromobenzoyl, 4-nitrobenzoyl, 4-tert-butylbenzoyl, 4-chlorobenzoyl, and 3-chlorobenzoyl) groups were subjected to modification of hydroxyl (–OH) group of MDG to observe the variation in biological activities.

The modified MDG esters **4** and **10**, which contained the maximum numbers of heavy and rotatable atoms, exhibited excellent antibacterial activity in PASS and molecular docking analysis.

Table 1

Chemical structural views of MDG esters with SMILES

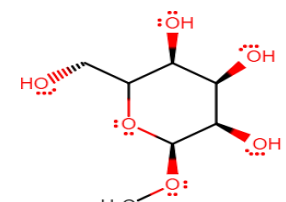
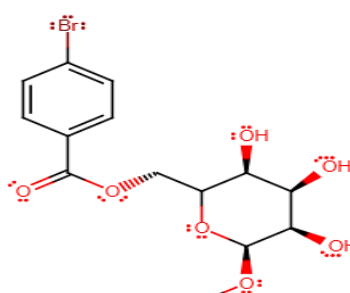
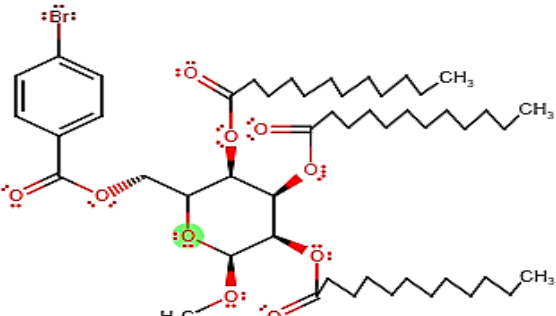
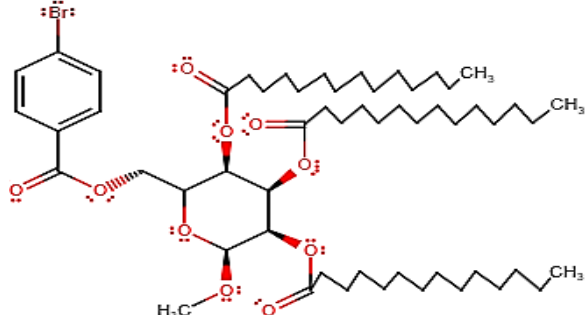
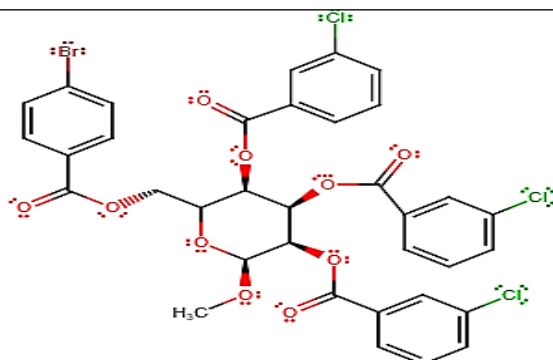
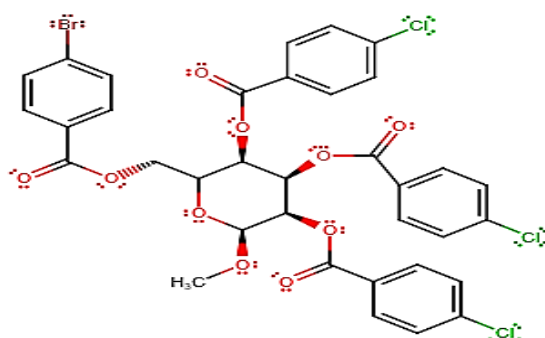
Compound	Chemical structure	SMILES
1	 <p>Methyl β-D-galactopyranoside</p>	<chem>COC1OC(CO)C(O)C(O)C1O</chem>
2	 <p>Methyl 6-<i>O</i>-(4-bromobenzoyl)-β-D-galactopyranoside</p>	<chem>COC1OC(COC(=O)C2=CC=C(Br)C=C2)C(O)C(O)C1O</chem>
3	 <p>Methyl 6-<i>O</i>-(4-bromobenzoyl)-2,3,4-tri-<i>O</i>-lauroyl-β-D-galactopyranoside</p>	<chem>CCCCCCCCCCCC(=O)OC1C(COC(=O)C2=CC=C(Br)C=C2)OC(OC)C(OC(=O)CCCCCCCCCCC)C1OC(=O)CCCCCCCCCCC</chem>
4	 <p>Methyl 6-<i>O</i>-(4-bromobenzoyl)-2,3,4-tri-<i>O</i>-myristoyl-β-D-galactopyranoside</p>	<chem>CCCCCCCCCCCCCCCC(=O)OC1C(COC(=O)C2=CC=C(Br)C=C2)OC(OC)C(OC(=O)CCCCCCCCCCC)C1OC(=O)CCCCCCCCCCC</chem>

Table 1 - continues

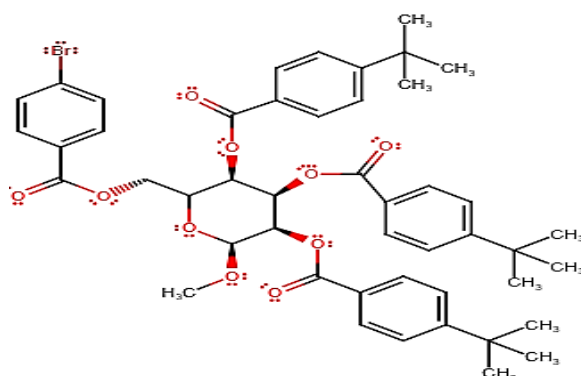
5

Methyl 6-*O*-(4-bromobenzoyl)-2,3,4-tri-*O*-(3-chlorobenzoyl)-β-D-galactopyranoside
COC1OC(COC(=O)C2=CC=C(Br)C=C2)C(OC(=O)C2=CC=C(Cl)=CC=C2)C(OC(=O)C2=CC(Cl)=CC=C2)C1OC(=O)C1=CC=CC(Cl)=C1

6

Methyl 6-*O*-(4-bromobenzoyl)-2,3,4-tri-*O*-(4-chlorobenzoyl)-β-D-galactopyranoside
COC1OC(COC(=O)C2=CC=C(Br)C=C2)C(OC(=O)C2=CC=C(Cl)C=C2)C(OC(=O)C2=CC=C(Cl)C=C2)C1OC(=O)C1=CC=C(Cl)C=C1

7

Methyl 6-*O*-(4-bromobenzoyl)-2,3,4-tri-*O*-(4-*t*-butylbenzoyl)-β-D-galactopyranoside
COC1OC(COC(=O)C2=CC=C(Br)C=C2)C(OC(=O)C2=CC=C(C(C)(C)C)C=C2)C(OC(=O)C2=CC=C(C(C)(C)C)C=C2)C1OC(=O)C1=CC=C(C(C)(C)C)C=C1

8

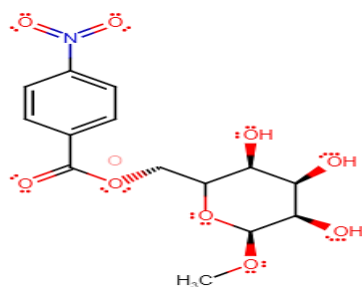
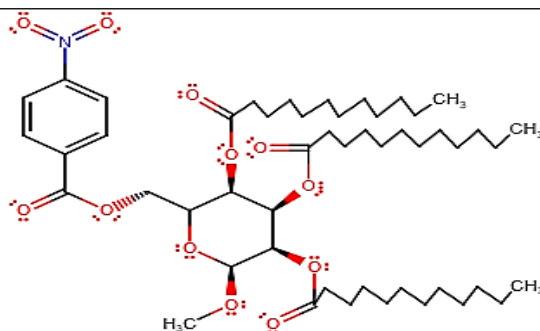
Methyl 6-*O*-(4-nitrobenzoyl)-β-D-galactopyranoside
COC1OC(COC(=O)C2=CC=C(C(=O)N(=O)=O)C=C2)C(O)C(O)C1O

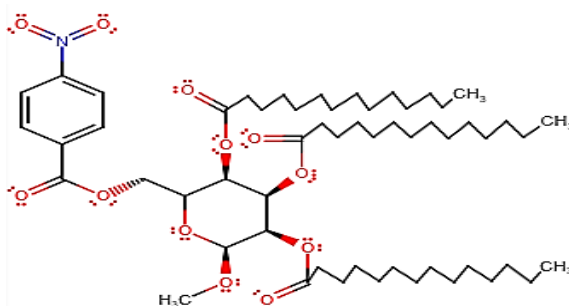
Table 1 - continues

9

Methyl 2,3,4-tri-*O*-lauroyl-6-*O*-(4-nitrobenzoyl)-β-D-galactopyranoside

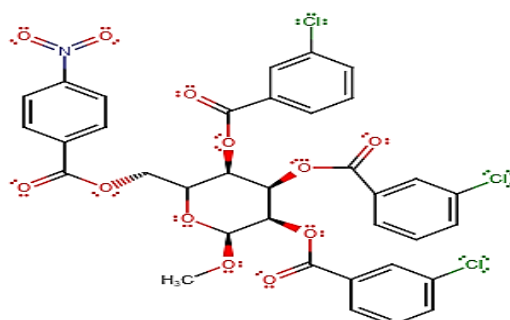
```
CCCCCCCCCCCC(=O)OC1C
(COC(=O)C2=CC=C(C=C2)N
(=O)=O)OC(OC)C(OC(=O)CCC
CCCCCCCC)C1OC(=O)CCCC
CCCCC
```

10

Methyl 2,3,4-tri-*O*-myristoyl-6-*O*-(4-nitrobenzoyl)-β-D-galactopyranoside

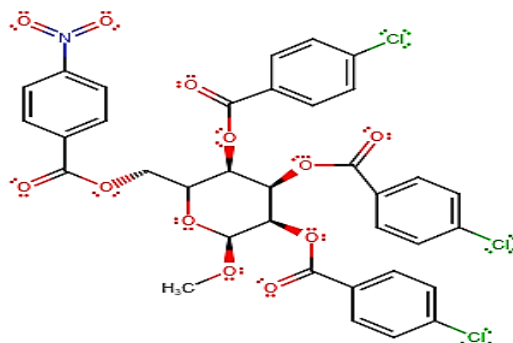
```
CCCCCCCCCCCCCCCC(=O)OC1
C(COC(=O)C2=CC=C(C=C2)N
(=O)=O)OC(OC)C(OC(=O)CCC
CCCCCCCC)C1OC(=O)CC
CCCCCCCC
```

11

Methyl 2,3,4-tri-*O*-(3-chlorobenzoyl)-6-*O*-(4-nitrobenzoyl)-β-D-galactopyranoside

```
COC1OC(COC(=O)C2=CC=C
(C=C2)N(=O)=O)C(OC(=O)C2=
CC=CC(Cl)=C2)C(OC(=O)C2=
CC(Cl)=CC=C2)C1OC(=O)C1=
CC(Cl)=CC=C1
```

12

Methyl 2,3,4-tri-*O*-(4-chlorobenzoyl)-6-*O*-(4-nitrobenzoyl)-β-D-galactopyranoside

```
COC1OC(COC(=O)C2=CC=C
(C=C2)N(=O)=O)C(OC(=O)C2=
CC=C(Cl)C=C2)C(OC(=O)C2=
CC=C(Cl)C=C2)C1OC(=O)C1=
CC=C(Cl)C=C1
```

Table 2

Molecular formula, formula weight and atomic identifications of MDG esters

Compounds	Molecular formula	Formula weight	Number of heavy atoms	Number of aromatic heavy atoms	Number of rotatable atoms	Number of H-bond acceptors	Number of H-bond donors
1	C ₇ H ₁₄ O ₆	194.18	13	0	2	6	4
2	C ₁₄ H ₁₇ O ₇ Br	377.18	22	6	5	7	3
3	C ₅₀ H ₈₃ O ₁₀ Br	924.09	61	6	41	10	0
4	C ₅₆ H ₉₅ O ₁₀ Br	1008.25	65	6	45	10	0
5	C ₃₅ H ₂₆ O ₁₀ BrCl ₃	792.84	49	24	14	10	0
6	C ₃₅ H ₂₆ O ₁₀ BrCl ₃	792.84	49	24	14	10	0
7	C ₄₇ H ₅₃ O ₁₀ Br	857.82	58	24	17	10	0
8	C ₁₄ H ₁₇ O ₉ N	343.29	24	6	6	9	3
9	C ₅₀ H ₈₃ O ₁₂ N	890.19	62	6	41	12	0
10	C ₅₆ H ₉₅ O ₁₂ N	974.35	68	6	47	12	0
11	C ₃₅ H ₂₆ O ₁₂ NCl ₃	758.94	51	24	15	12	0
12	C ₃₅ H ₂₆ O ₁₂ NCl ₃	758.94	51	24	15	12	0

3.2. Evaluation of antimicrobial activities: PASS

The prediction of antimicrobial spectrum was performed by applying the PASS web server to all the MDG esters 2–12. The PASS results are quoted as Pa and Pi and are displayed in Table 3. It was manifest from Table 3 that MDG esters 2–12 showed $0.60 < Pa < 0.69$ for antibacterial, $0.47 < Pa < 0.55$ for antifungal, $0.29 < Pa < 0.43$ for antioxidant and $0.29 < Pa < 0.56$ for anti-carcinogenic activities. These results revealed that these molecules were more efficient against bacteria than

against fungal pathogens. Attachment of additional aliphatic acyl chains (C12 to C14) increased antibacterial activity ($Pa = 0.669$) of MDG 1 ($Pa = 0.669$), and the insertion of Cl- and Br-substituted aromatic groups also resulted in reasonable improvements. The same scenario was observed for antioxidant activity, where acyl chain esters revealed improved values over the halo-benzoyl esters. However, ester 8, which has the 4-nitrobenzoyl group, exhibited the highest antioxidant activity ($Pa = 0.433$). We also tried to predict the anti-carcinogenic parameter of these esters.

Table 3

Prediction of antimicrobial activity of the MDG esters using PASS

Compounds	Antimicrobial activity							
	Antibacterial		Antifungal		Antioxidant		Anti-carcinogenic	
	Pa	Pi	Pa	Pi	Pa	Pi	Pa	Pi
1	0.541	0.013	0.628	0.016	0.667	0.004	0.765	0.005
2	0.633	0.015	0.507	0.016	0.441	0.009	0.546	0.023
3	0.669	0.012	0.529	0.014	0.340	0.018	0.557	0.040
4	0.669	0.012	0.529	0.014	0.340	0.018	0.557	0.040
5	0.614	0.017	0.514	0.024	0.294	0.024	0.549	0.085
6	0.617	0.017	0.518	0.021	0.314	0.021	0.554	0.062
7	0.618	0.017	0.529	0.021	0.402	0.012	0.536	0.046
8	0.630	0.015	0.538	0.013	0.433	0.013	0.561	0.043
9	0.666	0.012	0.558	0.012	0.336	0.018	0.383	0.034
10	0.666	0.012	0.558	0.012	0.336	0.018	0.383	0.034
11	0.609	0.018	0.471	0.019	0.292	0.024	0.292	0.062
12	0.612	0.017	0.488	0.018	0.306	0.018	0.315	0.053
Azithromycin	0.964	0.000	0.723	0.009	–	–	0.517	0.008

Therefore, PASS determination resulted in $0.29 < Pa < 0.56$ for anti-carcinogenicity, which revealed that the MDG esters had greater potential as anti-carcinogenic agents than as antimicrobials. Significantly, antibacterial, antifungal, antioxidant, and anti-carcinogenic properties of MDG esters with saturated acyl chains (**3**, **4** and **9**, **10**) were found more promising than the halo-benzoyl and 4-nitrobenzoyl esters (**5–8** and **11**, **12**).

3.3. Molecular docking studies

Protein synthesis occurs on macromolecular machines called ribosomes. Bacterial ribosomes and the translational machinery represent one of the main targets of antibiotics in the cell.³⁵

As a macromolecular docking target for the esters described in this report, we selected the macrolide enzyme phosphotransferase (MPH). The 2D structures of the synthesized ligand molecules were converted to energy-minimized 3D structures and further used for *in silico* protein–ligand docking. Excellent binding affinity is demonstrated by the minimal energy score needed for complex formation between the ligand and the receptor. Very low energy suggests the burying of the ligand in the receptor cavity. To compare the binding mode with a known drug, the reference ligand azithromycin was also docked at the same site of the MPH. All the sequences are displayed in Figure 2.

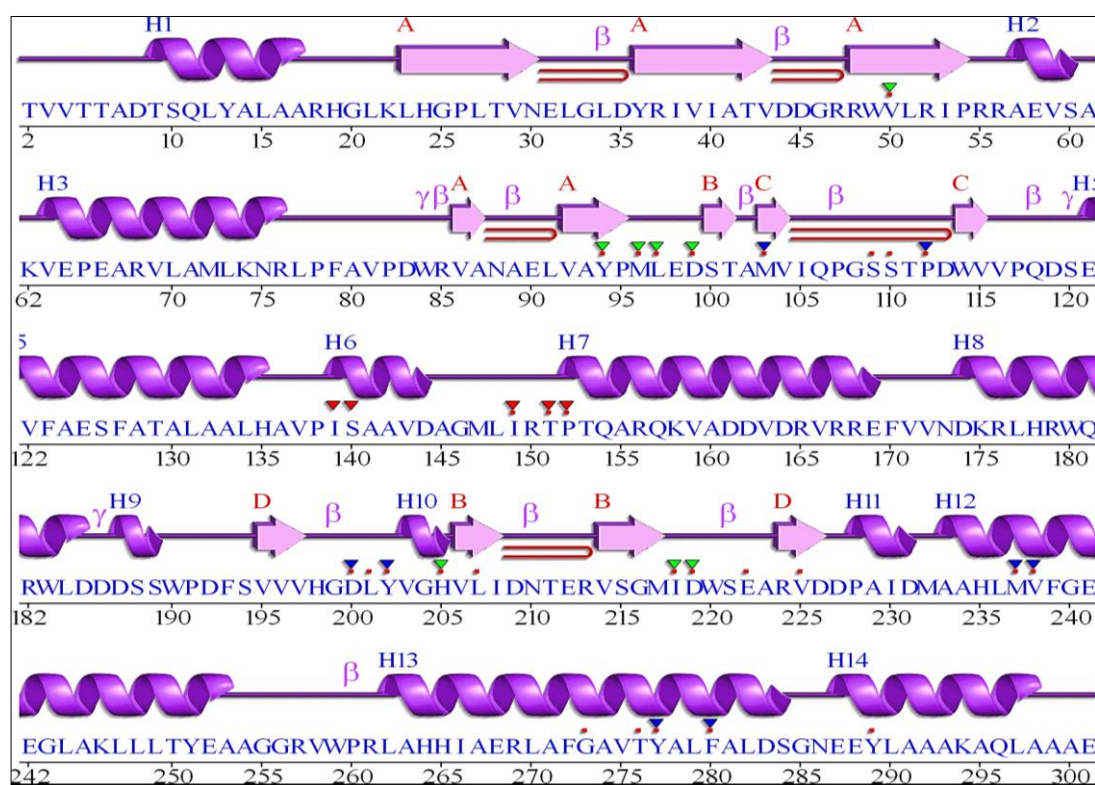


Fig. 2. Multiple sequence alignment of the closest homologs of MPH (PDB: 5igi)

All docked esters fitted in the active site of MPH and the resulting energy scores (*S*), as well as amino acid interactions, are listed in Figure 3 and Table 4. In all the docking poses, the chemical nature of the residues at the binding sites within 3 Å of the bound ligands were polar, positively charged residues (His205, Arg176, Arg269, and Arg224), aromatic hydrophobic residues (Tyr289, Tyr276, Tyr202, Phe280, and Phe272), and aliphatic hydrophobic residues (Leu201, Leu 32,

Leu97, Ala516, Ile230, Ile205, Ile218, Gly108 Asp200, Asp219, Gly33, Ser109, and Thr276). According to molecular docking analysis, the esters **3–7** and **9–12** favored ligands that had scoring ratings of -11.50 to -8.12 kcal/mol. The score value for the above-mentioned standard compound (azithromycin) was lower than those of our esters (binding energy -8.10 kcal/mol), reflecting that they could bind well with the receptor macrolide enzyme MPH.

Tyr289 and the binding interaction of azithromycin-5igi is not an exact match with that of MDG esters-5igi due to differences in the structure.

Although differing in size and varying in substitutions, the MDG esters bind to the MPH enzyme in a similar location, adopt similar conformations, and interact with the enzymes in a similar manner (Fig. 3). Analysis of the binding site revealed that the synthesized ligands are stabilized by a variety of favorable interactions including polar interactions and hydrogen bonds, and most were hydrophobic interactions (Table 5).

2D interactions of esters **5**, **9**, **11**, and **12**, presented in Figure 4a, showed that the ester car-

bonyl oxygen formed hydrogen bonds with Arg224, Tyr289, His205, and Asp200. These hydrogen-bond interactions are close enough to support di-substituted MDG fragments in the inner groove of the MPH active site. Hydrogen- and hydrophobic-bond surfaces of MPH (PDB: 5igi) with ester **10** are displayed in Figure 4b. The chain hydrocarbons in the R₂ position of esters **3** and **4** interact with side chains of the core subdomain and linker, including Tyr298, Thr276, Glu222, and Asp200 (Fig. 5). The phenyl ring (position R₂ of esters **10** and **11**) interacts with the helical subdomain of the C-terminal lobe, notably Phe280, Asp200, and Glu222 (Fig. 5).

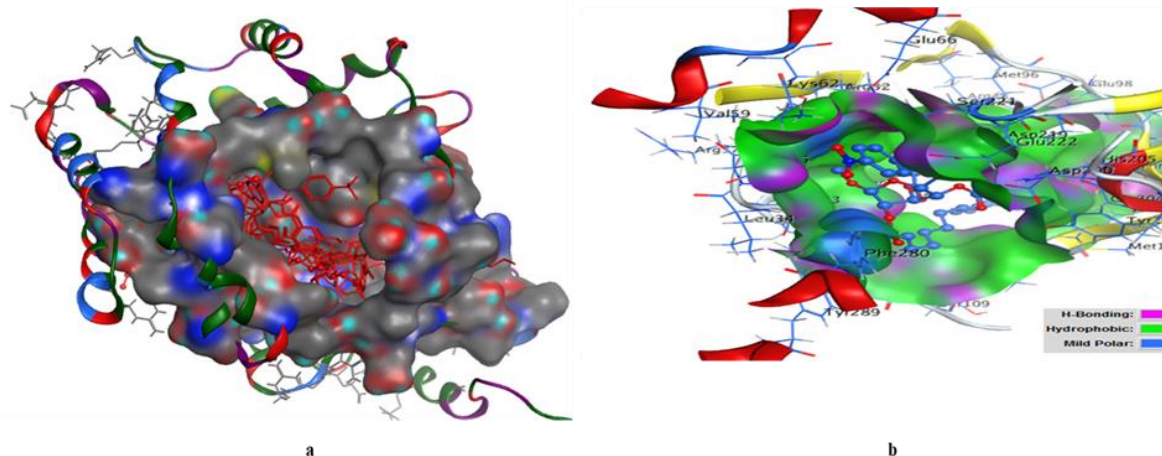


Fig. 4. (a) The synthesised esters in the active sites of type I macrolide 2'-phosphotransferase (PDB: 5igi); and (b) Hydrogen- and hydrophobic-bond surface of MPH (PDB: 5igi) with ester **10**

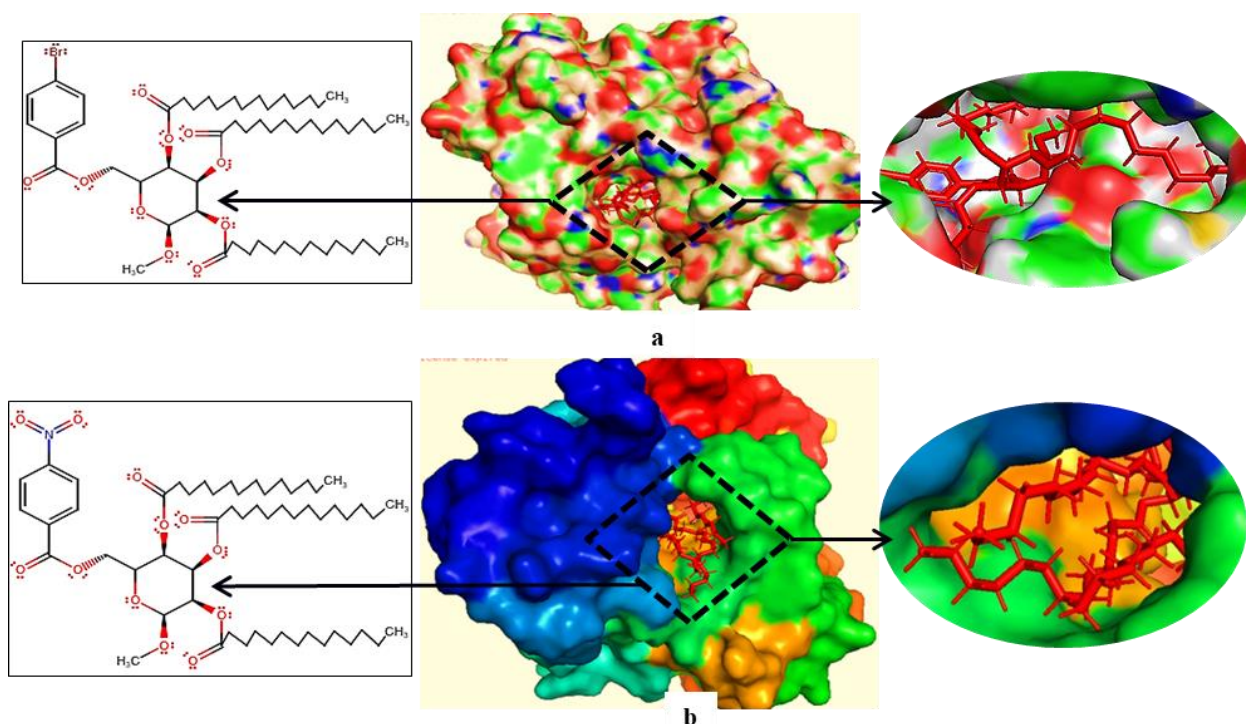


Fig. 5. (a) The docked 2D pose of ester **4** with MPH (PDB: 5igi) and (b) The docked 2D pose of ester **10** with MPH (PDB: 5igi)

The results of the antibacterial activity and docking studies revealed that the substitution of the hydroxyl group in position R₂ by bulky groups is favorable for increasing the antibacterial activity; this could be explained by the hydrophobic interactions in the MPH active site (Fig. 5). Comparison of results of esters **1**, **3**, and **6** shows the apparent

dependency between inhibition potency of these compounds and their propensity to bind to this pocket. From the docking study, we predicted that MDG esters **3–7** and **9–12** would possess better antibacterial activity than the standard drug due to the good binding affinity with the target protein and could be used as potential antimicrobial drugs.

Table 5

Molecular docking, binding scores, and binding interaction of the synthase esters and the standard drug azithromycin in the active sites of type I macrolide 2'-phosphotransferase (PDB: 5igi)

Compounds	Binding energy (kcal/mol)	H-bond	Distance (Å)	Interaction hydrophobic
3	-10.11	Lys158 Arg224 Arg269	2.81 3.30 2.90	Phe280, Thr276, Asp200, Gly273, Gly199, Phe272, Ile230, Arg150, Glu22, Asp35, Tyr289
4	-11.11	Tyr289	3.17	Phe280, Thr276, Asp200, Ile38, Arg224, Glu22, Asp35, Tyr289, His205, Tyr202, Ile40, Thr28, Tyr277, Arg269
5	-8.31	Tyr289	3.35	Phe280, Asp200, Ser221, Tyr36, Arg52, His205, Asp219, Asn30, Gly33, Ile38, Ser109, Leu32, Glu222
7	-8.99	*****	***	Met273, Gln296, Tyr277, Thr276, Phe272, Gly199, Arg269, Arg224, Ala234, Asp200, Tyr202, Met103
9	-10.33	His205 asp200	2.97 2.97	Asp219, Asn30, Gly33, Ile38, Ser109, Leu32, Glu222, Leu279, Glu22, Asp162, Tyr36, Met96, Thr101
10	-11.51	Ile105	2.90	Phe280, Asp200, Ser221, Tyr36, Arg52, His205, Asp219, Thr101, Tyr202, Ile218, Thr28, Tyr277, Met108
11	-8.11	Tyr202	3.61	Leu201, Tyr277, Thr277, Thr276, Asp200, Glu222, Phe280, Asp25
12	-8.64	Arg224	3.06	Phe280, Thr276, Asp200, Glu22, Asp35, Ser221, Tyr36, Arg269, Lys158, Lys62
Azithromycin	-8.10	Tyr289	3.59	Gly204, Met103, Ser109, Gln10, Ile105, Tyr202, Gly108, Tyr3, Asp209, Phe280, Arg52

NB; Tyr = Tyrosine, Cys = Cysteine, Gly = Glycine, His = Histidine, Arg = Arginine, Leu = Leucine, Met = Methionine, Ile = Isoleucine, Ala = Alanine, Asn = Asparagine, Thr = Threonine, Ser = Serine, Gln = Glutamine, Phe = Phenylalanine, Lys = Lysine, Glu = Glutamic acid, Asp = Aspartic acid.

3.4. Prediction of the pharmacokinetic properties and toxicity

In an attempt to predict the pharmacokinetic properties such as the ADMET of the compounds, we used the pkCSM ADMET descriptors algorithm protocol. Drug absorption depends on various factors, including membrane permeability [indicated by the cell line of colon cancer (Caco-2)], intestinal absorption, skin permeability thresholds, substrate or inhibition of P-glycoprotein. A value of intestinal absorbance below 30 % suggests poor absorbance. According to the results in Table 6, all compounds show excellent absorption, with absorption values of >30.

Skin permeability is an important consideration in improving drug efficacy and is of particular interest in the development of transdermal drug delivery. A molecule will barely penetrate the skin if logK_p is >-2.5 cm/h.³⁵ From Table 6 it can be seen that the skin permeabilities, K_p, of all MDG esters were -2.731 cm/h (<-2.5). Therefore, it can be predicted that all derivatives would show good skin penetrability. For the pkCSM predictive model, high Caco-2 permeability is translated into predicted logP_{app} values of >0.90 cm/s.³⁵ As Table 6 shows, the value of Caco-2 permeability (log P_{app}) of the MDG esters ranged from -4.1 to -2.3 cm/s, i.e., logP_{app} < 0.9 cm/s, so it is predicted that these have low Caco-2 permeability.

Table 6

In silico prediction of absorption of MDG esters

Compounds	Water solubility (log mol/l)	Caco-2 permeability	Intestinal absorption	Skin permeability
3	-2.931	0.850	100	-2.735
4	-2.735	0.778	100	-2.735
5	-2.931	0.850	100	-2.735
7	-2.892	-0.691	100	-2.735
9	-2.91	-0.691	100	-2.735
10	-2.89	-0.852	100	-2.735
11	-2.952	0.486	88.709	-2.735
12	-2.962	0.486	88.691	-2.735

In the discovery of orally administered drugs, solubility is one of the major descriptors. High water solubility is useful for delivering active ingredients in sufficient quantity in a small volume of pharmaceutical dosage. The values of water solubility are given in log(mol/l) (insoluble ≤ -10 < poorly soluble < -6 < moderately soluble < -4 < soluble < -2 < very soluble < $0 \leq$ highly soluble).^{36–38} The results are shown in Table 6 and suggest that the tested esters are soluble.

Distribution volume (Vd) is a pharmacokinetic parameter reflecting the tendency of an individual substance to either linger in the plasma or to be re-distributed to another tissue compartment. According to Pires *et al.*³⁵ VDss is considered low if it is below 0.71 l/kg (log VDss < -0.15) and high if it is above 2.81 l/kg (log VDss > 0.45); it is shown in Table 7 that the VDss-value of MDG esters ranged from -1.66 to -0.7 , with only one compound having a VDss-value of < -0.15 (ester 7).

Table 7

In silico prediction of distribution and excretion of MDG esters

Compounds	Distribution			Excretion	
	Vdss	BBB permeability	CNS permeability	Total clearance	Renal OCT2 substrate
3	-0.964	-2.382	-1.932	0.987	No
4	-1.492	-2.511	-1.862	1.178	No
5	-0.964	-2.361	-1.944	0.955	No
7	-0.014	-4.900	-1.782	0.500	No
9	-1.288	-2.697	-2.096	1.668	No
10	-1.661	-2.827	-2.026	-1.761	No
11	-0.784	-2.627	-2.551	-0.114	No
12	-0.784	-2.627	-2.551	-0.114	No

The blood–brain partitioning and brain distribution are critical properties for drugs targeting the central nervous system. Compounds showing logBB < -1 are considered poorly distributed in the brain. From Table 7 it can be seen that the logPS (the central nervous system, CNS, permeability) value of MDG esters ranges from -1.7 to -2.5 , i.e., logPS < -3 which predicts that all derivatives of the compound would be unable to penetrate the CNS. It can be seen in Table 7 the log

CLtot value of MDG esters ranges from -1.7 to 1.6 ml/min/kg; from those values can be predicted the rate of excretion of the compound. Metabolism is considered based on the CYP models for substrate or inhibition (CYP2D6, CYP1A2, CYP2C19, and CYP3A4). It was established (Table 8) that all MDG esters do not affect or inhibit all the enzymes, so it can be concluded that all the esters tend to be metabolized in the body by the P450 enzyme.

Table 8

In silico prediction of metabolism of MDG esters

Compounds	Cyp1A2	Cyp2C19	Cyp2D6	Cyp3A4
3	No	No	No	No
4	No	No	No	No
5	No	No	No	No
7	No	No	No	No
9	No	No	No	No
10	No	No	No	No
11	No	No	No	No
12	No	No	No	No

The model provided by pkCSM pharmacokinetics predicts the total clearance log(CL_{tot}) of a given compound in log(ml/min/kg). The larger the CL_{tot} value of the compound, the faster the excretion processes. The results for the esters are described in Table 9, and their high LD50 values (2.3–2.5) suggest that they are lethal only in very high doses. The negative result in the AMES test suggests that the compounds could not be mutagenic. The results also suggest that all compounds tested may not inhibit the hERG channel and may not cause skin sensitization.

Table 10

Drug-likeness prediction of the MDG esters based on Lipinski, Muegge Ghose, Veber, and Egan

Compounds	Molecular weights	HBA	Lipinski	Muegge	Veber	Egan	Ghose
1	194.18	6	Yes	No	Yes	Yes	No
2	377.18	7	Yes	Yes	Yes	Yes	Yes
3	924.09	10	No	No	No	No	No
4	1008.25	10	No	No	No	No	No
5	792.84	10	No	No	No	No	No
6	792.84	10	Yes	Yes	No	No	No
7	857.82	10	Yes	Yes	No	No	No
8	343.29	9	Yes	Yes	No	No	No
9	890.19	12	No	No	No	No	No
10	974.35	12	No	No	No	No	No
11	758.94	12	Yes	Yes	No	No	No
12	758.94	12	Yes	Yes	No	No	No
Azithromycin			No	No	No	No	No

HBA = Hydrogen-bond acceptor

However, topological polar surface area (TPSA) is likewise employed as a contributing factor for oral absorption and blood–brain barrier permeation capacity; the screened drug-likeness of a molecule should have a TPSA of 20–130 Å². The SwissADME web tool prediction revealed that only esters **8–12** violated this TPSA standard and all

Table 9

In silico prediction of toxicity of MDG esters

Compounds	Ames toxicity	Herg1 inhibition	LD50	Skin sensitisation
3	No	No	2.392	No
4	no	no	2.442	no
5	No	No	2.375	No
7	No	No	2.482	No
9	No	No	2.403	No
10	No	No	2.458	No
11	No	No	2.522	No
12	No	No	2.522	No

LD50 = Lethal Dose 50 (oral rat acute toxicity; mol/kg)

The modified MDG esters were also evaluated with the SwissADME web tool for their drug-likeness, which is crucial for rational drug design. Generally, drug-likeness is evaluated using Lipinski's rule of five.³⁹ The MDG esters **2** and **8** fulfill all the conditions of Lipinski's rule of five (Tables 10 and 11).

others esters **2–7** are anticipated to be orally bioavailable. In addition, Pan-assay Interference (PAINS) tests revealed no violation by these MDG esters. PAINS are chemical compounds that often give false-positive results in high-throughput screens.

Table 11

Lipinski's properties of modified MDG esters

Compounds	Synthetic accessibility	Bioavailability score	PAINS alert	TPSA (Å ²)	Csp3	Molar refractivity
1	4.30	0.55	0	99.38	1.00	40.47
2	4.15	0.55	0	105.45	0.50	77.80
3	8.49	0.17	0	123.66	0.80	251.23
4	9.04	0.17	0	123.66	0.81	270.45
5	5.04	0.17	0	123.66	0.20	181.75
6	5.48	0.17	0	123.66	0.20	181.75
7	6.99	0.17	0	123.66	0.40	224.53
8	4.17	0.55	0	151.27	0.50	78.93
9	8.9	0.17	0	169.48	0.80	247.54
10	9.22	0.17	0	169.48	0.82	276.38
11	5.58	0.17	0	169.48	0.20	182.87
12	5.52	0.17	0	169.48	0.20	182.87
Azithromycin	8.91	0.17	0	108.08	0.97	8.91

Csp3 = "the ratio of sp³ hybridized carbons over the total carbon count of the molecule (Fraction Csp3)"

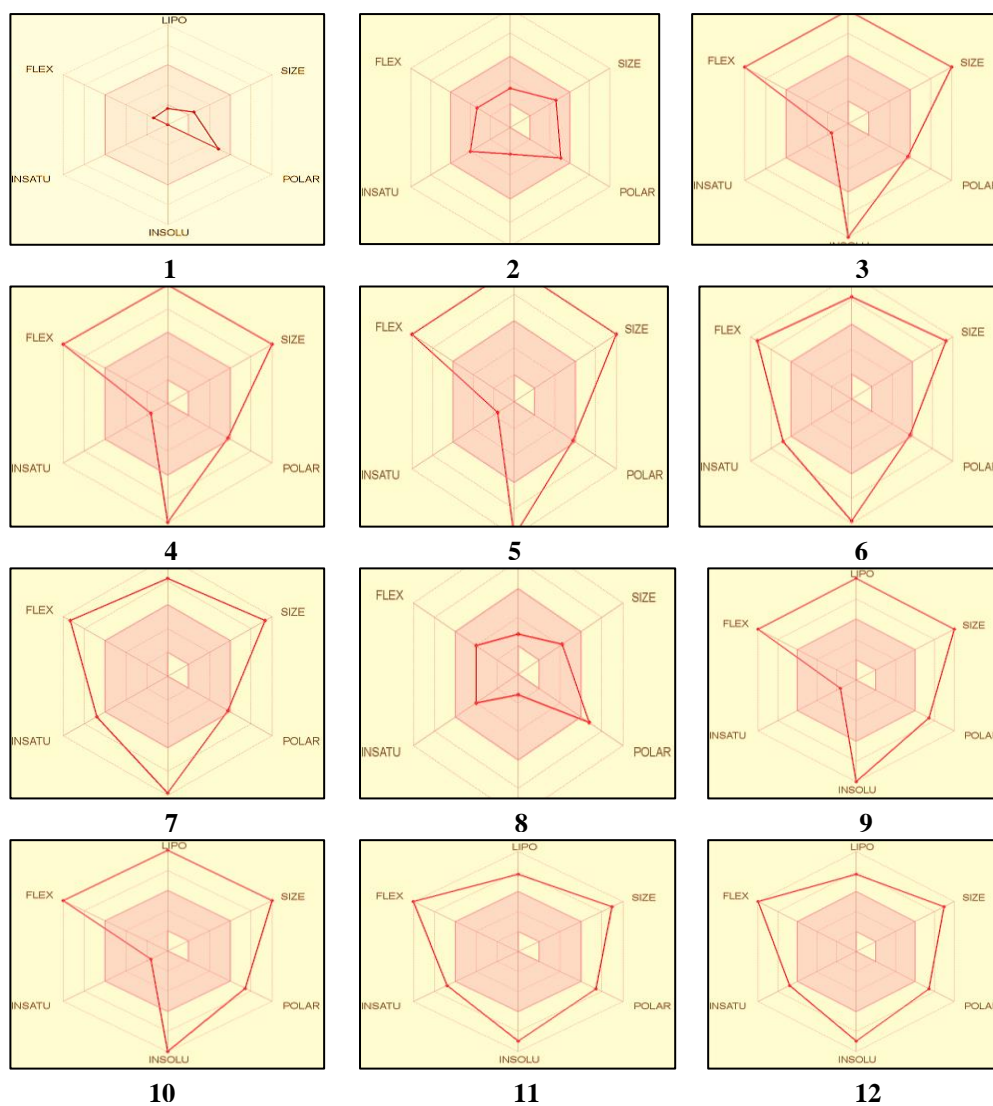


Fig. 6. Bioactivity radar charts of the MDG esters, where FLEX: flexibility, LIPO: lipophilicity, INSATU: insaturation, and INSOLU: insolubility

Therefore, all new MDG esters designed showed a somewhat standard value and were acceptable regarding the persistence of the drug in the body. Moreover, it is necessary to examine whether the predicted compounds are nontoxic because this plays a critical role in drugs selection. Bioactivity radar charts of the MDG esters (Fig. 6) revealed the promising pharmacokinetic profiles of all candidates. Overall, the new molecules designed present good pharmacokinetic properties. The designed esters were also evaluated for their synthetic accessibility, and the synthetic accessibility values for all designed MDG esters were between **4** and **9**; therefore, it may be suggested that they are easily synthesized.

4. CONCLUSIONS

In this study, several monosaccharide fatty-acid, (i.e., MDG), esters were analyzed successfully *in silico* for their antimicrobial, molecular docking, pharmacokinetic, drug-likeness, and toxicity properties. Insertion of various aliphatic and aromatic groups in the MDG structure could significantly improve their biological activity mode. PASS predictions of the MDG esters **2–12** were $0.60 < Pa < 0.69$ for antibacterial and $0.47 < Pa < 0.55$ for antifungal activity which revealed the antibacterial potency of the modified esters. However, molecular docking was effectively employed to suggest the best antibacterials against macrolide phosphotransferase enzyme MPH. The MDG esters showed an interesting range of binding affinity, of -5.50 to -11.51 kcal/mol, and including several non-covalent interactions, such as hydrogen-bonding, hydrophobic, and electrostatic interactions. These blind molecular docking analyses may provide a potential approach for the application of antibacterial drugs as expected inhibitors of macrolide phosphotransferase enzyme MPH. Finally, these esters were analyzed for their pharmacokinetic properties, which revealed that the combination of toxicity prediction, *in silico* ADMET prediction, and drug-likeness were promising because most of the designed molecules showed improved kinetic parameters and conformed to all drug-likeness rules as well as presenting interesting results in terms of biological activity. So, it could be concluded that most of the antibacterials showed promise and could be used in the design of effective antibacterial drugs against macrolide phosphotransferase enzyme MPH. In this promising investigation, more *in vitro* and *in vivo* drug-likeness studies, such as nontoxic concentration

toward healthy cells, may be conducted in the near future.

Author contributions. Sarkar M. A. Kawsar: methodology, article writing, results monitoring, and supervision of experimental results; Mebarka Ouassaf: interpretation of experimental results and performance of computational works; Samir Chtita: article writing and interpretation of DFT calculations; Aishi B. Jui: interpretation of experimental results and analysis; and Salah Belaidi: results monitoring, validation of results, and validation of the article.

Conflict of interests. The authors declare that they have no known competing financial interests or personal relationships that could have appeared to influence the work reported in this paper.

Acknowledgment. This work was supported by the Ministry of Science and Technology of People's Republic of Bangladesh (No. 39.00.0000.009.06.009.20-1331/Phy's-530).

REFERENCES

- [1] Tyers, M.; Wright, G. D. Drug combinations: A strategy to extend the life of antibiotics in the 21st Century. *Nature Rev. Microbiol.* **2019**, *17* (3), 144–155. <https://doi.org/10.1038/s41579-018-0141-x>.
- [2] Amin, M. R.; Yasmin, F.; Hosen, M. A.; Dey, S.; Mahmud, S.; Saleh, M. A.; Hasan, I.; Fujii, Y.; Yamada, M.; Ozeki, Y.; Kawsar, S. M. A. Synthesis, antimicrobial, anticancer, PASS, molecular docking, molecular dynamic simulations and pharmacokinetic predictions of some methyl β -D-galactopyranoside analogs. *Molecules* **2021**, *26* (22), 1–25. <https://doi.org/10.3390/molecules26227016>.
- [3] Amin, M. R.; Yasmin, F.; Dey, S.; Mahmud, S.; Saleh, Emran, T. B.; Hasan, I.; Rajia, S.; Ogawa, Y.; Fujii, Y.; Yamada, M.; Ozeki, Y.; Kawsar, S. M. A. Methyl β -D-galactopyranoside esters as potential inhibitors for SARS-CoV-2 protease enzyme: synthesis, antimicrobial, PASS, molecular docking, molecular dynamics simulations and quantum computations. *Glycoconjugate J.* **2021**, *38* (5), 1–30. <https://doi.org/10.1007/s10719-021-10039-3>.
- [4] Tong, S. Y.; David, J. S.; Eichenberger, E.; Holland, T. L.; Fowler, V. G. J. *Staphylococcus aureus* infections: epidemiology, pathophysiology, clinical manifestations, and management. *Clin. Microbiol. Rev.* **2015**, *28* (3), 603–661. <https://doi.org/10.1128/cmr.00134-14>.
- [5] Noble, S. M.; Gianetti B. A.; Witchley, J. N. *Candida albicans* cell-type switching and functional plasticity in the mammalian host. *Nat. Rev. Microbiol.* **2017**, *15* (2), 96–108. <https://doi.org/10.1038/nrmicro.2016.157>.
- [6] Hosen, M. A.; Alam, A.; Islam, M.; Fujii, Y.; Ozeki, Y.; Kawsar, S. M. A. Geometrical optimization, PASS prediction, molecular docking, and in silico ADMET studies of thymidine derivatives against FimH adhesin of *Escherichia coli*. *Bulg. Chem. Commun.* **2021**, *53* (3), 327–342. <http://doi.org/10.34049/bcc.53.3.5375>.
- [7] Golkar, T.; Zeliński, M.; Berghuis, A. B. Look and outlook on enzyme-mediated macrolide resistance. *Front. Microbiol.* **2018**, *9* (1942), 1–15. <https://doi.org/10.3389/fmicb.2018.01942>.

- [8] Noreen, N. K.; Daniel, C. J.; Zarek, S. S. Synthesis, kinetics and inhibition of Escherichia coli Heptosyltransferase I by monosaccharide analogues of Lipid A. *Bioorg. Med. Chem. Lett.* **2018**, *28* (4), 594–600. <https://doi.org/10.1016/j.bmcl.2018.01.040>.
- [9] Kawsar, S. M. A.; Faruk, M. O.; Rahman, M. S.; Fujii, Y.; Ozeki Y. Regioselective synthesis, characterization, and antimicrobial activities of some new monosaccharide derivatives. *Sci. Pharm.* **2014**, *82* (1), 1–20. <https://doi.org/10.3797/scipharm.1308-03>.
- [10] Misbah, M. M. H.; Ferdous, J.; Bulbul, M. Z. H.; Chowdhury, T. S.; Dey, S.; Hasan, I.; Kawsar, S. M. A. Evaluation of MIC, MBC, MFC and anticancer activities of acylated methyl β -D-galactopyranoside Esters. *Int. J. Biosci.* **2020**, *16* (4), 299–309. <https://doi.org/10.12692/ijb/16.4.299-309>.
- [11] Mirajul, M. I.; Arifuzzaman, M.; Monjur, M. R.; Atiar, M. R.; Kawsar, S. M. A. Novel methyl 4,6-O-benzylidene- α -D-glucopyranoside derivatives: synthesis, structural characterization and evaluation of antibacterial activities. *Haceteppe J. Biol. Chem.* **2019**, *47* (2), 153–164. <https://doi.org/10.15671/hjbc.622038>.
- [12] Yasmin, F.; Amin, M. R.; Hosen, M. A.; Bulbul, M. Z. H.; Dey, S.; Kawsar, S. M. A. Monosaccharide derivatives: synthesis, antimicrobial, PASS, antiviral and molecular docking studies against SARS-COV-2 M^{PRO} inhibitors. *Cellu. Chem. Technol.* **2021**, *55* (5-6), 477–499. <https://doi.org/0.1126/science.1059820>
- [13] Bertozzi C. R.; Kiessling, L. L. Chemical Glycobiology. *Science* 2001, *291* (5512), 2357–2364. <https://doi.org/10.1126/science.1059820>.
- [14] Chen S.; Fukuda, M. Cell type-specific roles of carbohydrates in tumor metastasis. *Meth. Enzymol.* **2006**, *416*, 371–380. [https://doi.org/10.1016/S0076-6879\(06\)16024-3](https://doi.org/10.1016/S0076-6879(06)16024-3).
- [15] Kawsar, S. M. A.; Hamida, A. A.; Sheikh, A. U.; Hossain, M. K.; Shagir, A. C.; Sanallah, A. F. M.; Manchur, M. A.; Imtiaj, H.; Ogawa, Y.; Fujii, Y.; Koide, Y.; Ozeki, Y. Chemically modified uridine molecules incorporating acyl residues to enhance antibacterial and cytotoxic activities. *Int. J. Org. Chem.* **2015**, *5* (4), 232–245. <https://doi.org/10.4236/ijoc.2015.54023>.
- [16] Shagir, A. C.; Bhuiyan, M. M. R.; Ozeki Y.; Kawsar, S. M. A. Simple and rapid synthesis of some nucleoside derivatives: structural and spectral characterization. *Curr. Chem. Lett.* **2016**, *5* (2), 83–92. <https://doi.org/10.5267/j.ccl.2015.12.001>.
- [17] Kawsar, S. M. A.; Islam, M.; Jesmin, S.; Manchur, M. A.; Hasan, I.; Rajia, S. Evaluation of the antimicrobial activity and cytotoxic effect of some uridine derivatives. *Int. J. Biosci.* **2018**, *12* (6), 211–219. <https://doi.org/10.12692/ijb/12.6.211-219>.
- [18] Rana, K. M.; Ferdous, J.; Hosen, A.; Kawsar, S. M. A. Ribose moieties acylation and characterization of some cytidine analogs. *J. Sib. Fed. Univ. Chem.* **2020**, *13* (4), 465–478. <https://doi.org/10.17516/1998-2836-0199>.
- [19] Bulbul, M. Z. H.; Chowdhury, T. S.; Misbah, M. M. H.; Ferdous, J.; Dey, S.; Hasan, I.; Fujii, Y.; Ozeki, Y.; Kawsar, S. M. A. Synthesis of new series of pyrimidine nucleoside derivatives bearing the acyl moieties as potential antimicrobial agents. *Pharmacia* **2021**, *68* (1), 23–34. <https://doi.org/10.3897/pharmacia.68.e56543>.
- [20] Devi, S. R.; Jesmin, S.; Rahman, M.; Manchur, M. A.; Fujii, Y.; Kanaly, R. A.; Ozeki, Y.; Kawsar, S. M. A. Microbial efficacy and two step synthesis of uridine derivatives with spectral characterization. *Acta Pharm. Sci.* **2019**, *57* (1), 47–68. <https://doi.org/10.23893/1307-2080.APS.05704>.
- [21] Arifuzzaman, M.; Islam, M. M.; Rahman, M. M.; Mohammad, A. R.; Kawsar, S. M. A. An efficient approach to the synthesis of thymidine derivatives containing various acyl groups: characterization and antibacterial activities. *ACTA Pharm. Sci.* **2018**, *56* (4), 7–22. <https://doi.org/10.23893/1307-2080.APS.05622>.
- [22] Maowa, J.; Alam, A.; Rana, K. M.; Dey, S.; Hosen, A.; Fujii, Y.; Hasan, I.; Ozeki, Y.; Kawsar, S. M. A. Synthesis, characterization, synergistic antimicrobial properties and molecular docking of sugar modified uridine derivatives. *Ovidius Univ. Ann. Chem.* **2021**, *32* (1), 6–21. <https://doi.org/10.2478/auoc-2021-0002>.
- [23] Bulbul, M. Z. H.; Hosen, M. A.; Ferdous, J.; Chowdhury, T. S.; Misbah, M. M. H.; Kawsar, S. M. A. Thermochemical, DFT study, physicochemical, molecular docking and ADMET predictions of some modified uridine derivatives. *Int. J. New Chem.* **2021**, *8* (1), 88–110. <https://doi.org/10.22034/ijnc.2020.131337.1124>.
- [24] Maowa, J.; Hosen, M. A.; Alam, A.; Rana, K. M.; Fujii, Y.; Ozeki, Y.; Kawsar, S. M. A. Pharmacokinetics and molecular docking studies of uridine derivatives as SARS-CoV-2 M^{PRO} inhibitors. *Phys. Chem. Res.* **2021**, *9* (3), 385–412. <https://doi.org/10.22036/pcr.2021.264541.1869>.
- [25] Alam, A.; Hosen, M. A.; Hosen, A.; Fujii, Y.; Ozeki, Y.; Kawsar, S. M. A. Synthesis, characterization, and molecular docking against a receptor protein FimH of *Escherichia coli* (4XO8) of thymidine derivatives. *J. Mex. Chem. Soc.* **2021**, *65* (2), 256–276. <https://doi.org/10.29356/jmcs.v65i1.1464>.
- [26] Kawsar, S. M. A.; Hosen, M. A. An optimization and pharmacokinetic studies of some thymidine derivatives. *Turkish Comp. Theo. Chem.* **2020**, *4* (2), 59–66. <https://doi.org/10.33435/tcandtc.718807>.
- [27] Kawsar, S. M. A.; Hosen, M. A.; Fujii, Y.; Ozeki, Y. Thermochemical, DFT, molecular docking and pharmacokinetic studies of methyl β -D-galactopyranoside esters. *J. Comput. Chem. Mol. Model.* **2020**, *4* (4), 452–462. <https://doi.org/10.25177/JCCMM.4.4.RA.10663>.
- [28] Kumaresan, S.; Senthilkumar, V.; Stephen, A. B. S. GC-MS analysis and PASS-assisted prediction of biological activity spectra of extract of *Phomopsis* sp. isolated from *Andrographis paniculata*. *World J. Pharm. Res.* **2015**, *4* (1), 1035–1053.
- [29] Frisch, M. J.; Trucks, G. W.; Schlegel, H. B.; Scuseria, G. E.; Robb, M. A.; Cheeseman, J. R.; Scalmani, G.; Barone, V.; Petersson, G. A.; Nakatsuji, H.; Li, X.; Caricato, M.; Marenich, A. V.; Bloino, J.; Janesko, B. G.; Gomperts, R.; Mennucci, B.; Hratchian, H. P.; Ortiz, J. V.; Izmaylov, A. F.; Sonnenberg, J. L.; Williams-Young, D.; Ding, F.; Lipparini, F.; Egidi, F.; Goings, J.; Peng, B.; Petrone, A.; Henderson, T.; Ranasinghe, D.; Zakrzewski, V. G.; Gao, J.; Rega, N.; Zheng, G.; Liang, W.; Hada, M.; Ehara, M.; Toyota, K.; Fukuda, R.; Hasegawa, J.; Ishida, M.; Nakajima, T.; Honda, Y.; Kitao, O.; Nakai, H.; Vreven, T.; Throssell, K.; Montgomery, J. A., Jr; Peralta, J. E.; Ogliaro, F.; Bearpark, M. J.; Heyd,

- J. J.; Brothers, E. N.; Kudin, K. N.; Staroverov, V. N.; Keith, T. A.; Kobayashi, R.; Normand, J.; Raghavachari, K.; Rendell, A. P.; Burant, J. C.; Iyengar, S. S.; Tomasi, J.; Cossi, M.; Millam, J. M.; Klene, M.; Adamo, C.; Cammi, R.; Ochterski, J. W.; Martin, R. L.; Morokuma, K.; Farkas, O.; Foresman, J. B.; Fox, D. J. *Gaussian 16, Revision C.01*; Gaussian, Inc., Wallingford CT, USA, **2016**.
- [30] Laskowski, R. A.; Swindells, M. B. LigPlot+: multiple ligand–protein interaction diagrams for drug discovery. *J. Chem. Inf. Model.* **2011**, *51* (10), 2778–2786. <https://doi.org/10.1021/ci200227u>.
- [31] Marvig, R. L.; Søndergaard, M. S. R.; Damkiær, S.; Høiby, N.; Johansen, H. K.; Molin, S.; Jelsbak, L. Mutations in 23S rRNA confer resistance against Azithromycin in *Pseudomonas aeruginosa*. *Antimicrob. Agents Chemother.* **2012**, *56* (8), 4519–4521. <https://doi.org/10.1128/AAC.00630-12>.
- [32] Fong, D. H.; Burk, D. L.; Blanchet, J.; Yan, A. Y.; Berghuis, A. M. Structural basis for kinase-mediated macrolide antibiotic resistance. *Structure* **2017**, *25* (5), 750–761. <https://doi.org/10.1016/j.str.2017.03.007>.
- [33] Marvin, ChemAxon. <https://chemaxon.com/products/marvin>.
- [34] Frank, J. The ribosome—a macromolecular machine par excellence. *Chem. Biol.* **2000**, *7* (6), R133–141. [https://doi.org/10.1016/S1074-5521\(00\)00127-7](https://doi.org/10.1016/S1074-5521(00)00127-7).
- [35] Pires, D. E. V.; Blundell, T. L.; Ascher, B. D. pkCSM: Predicting small-molecule pharmacokinetic and toxicity properties using graph-based signatures. *J. Med. Chem.* **2015**, *58* (9), 4066–4072. <https://doi.org/10.1021/acs.jmedchem.5b00104>.
- [36] Fouedjou, R. T.; Chtita, S.; Bakhouch, M.; Belaidi, S.; Ouassaf, M.; Djoumbissie, L. A.; Tapondjou, L. A.; Qais, F. A. Cameroonian medicinal plants as potential candidates of SARS-CoV-2 inhibitors. *J. Biomol. Struct. Dyn.* **2021**, *28*, 1–15. <https://doi.org/10.1080/07391102.2021.1914170>.
- [37] A. Alam, K. M. Rana, M. A. Hosen, S. Dey, B. Bezbaruah, S. M. A. Kawsar, Modified thymidine derivatives as potential inhibitors of SARS-CoV: PASS, in vitro antimicrobial, physicochemical and molecular docking studies, *Phys. Chem. Res.* **2022**, *10* (3), 391–409. <https://doi.org/10.22036/PCR.2022.317494.1996>.
- [38] Ouassaf, M.; Belaidi, S.; Mogren, M.; Mogren, A.; Chtita, S.; Khan, S.; Htar, T. A. Docking-scoring approach to identify effective antiviral 2,5-diaminobenzophenone derivatives against the main protease of SARS-CoV-2. *J. King Saud Univ. Sci.* **2021**, *33*, 101352. <https://doi.org/10.1016/j.jksus.2021.101352>.
- [39] Lipinski, C. A.; Lombardo, F.; Dominy, B. W.; Feeney, P. J. Experimental and computational approaches to estimate solubility and permeability in drug discovery and development. *Adv. Drug Deliv. Rev.* **2001**, *46*, 3–25. [https://doi.org/10.1016/s0169-409x\(00\)00129-0](https://doi.org/10.1016/s0169-409x(00)00129-0).